Philosophical Magazine, 2015
Vol. 95, Nos. 16–18, 1896–1906, http://dx.doi.org/10.1080/14786435.2014.926036

Strain-dependent transition of time-dependent deformation mechanism in single-crystal ZnO evaluated by spherical nanoindentation

Yong-Jae Kim, In-Chul Choi, Jung-A Lee, Moo-Young Seok and Jae-il Jang*

Division of Materials Science and Engineering, Hanyang University, Seoul, 133-791, Korea

(*Received 16 December 2013; accepted 11 May 2014*)

We have systematically explored the time-dependent plasticity of (0 0 0 1)-oriented ZnO single crystal through spherical indentation tests. Constant load indentation creep tests were performed in elastic strain and elastic–plastic strain regimes. In both regimes, creep indeed occurred at ambient temperature. With the observed quasi-steady-static strain rate, the stress exponent was found as ~1.361 for elastic contact regime and ~3.077 for elastic–plastic regime, suggesting predominant creep mechanism of diffusion and dislocation, respectively. This strain-dependent transition of creep mechanism is discussed in terms of possible factors affecting the creep in each regime.

Keywords: nanoindentation; ZnO; creep

1. Introduction

Single-crystal ZnO is one of the most attractive semiconducting materials in electronic and optoelectronic applications, promised by its large direct band gap (~3.4 eV) and high exciton binding energy (~60 meV) at room temperature [1,2]. Several other attractive characteristics such as optical transparency, piezoelectricity and the crystal-growth technology for high-quality bulk single crystal [1–5] have further enhanced the technological interests in this material. Tremendous efforts have been devoted to study synthesis technology and electrical/optical properties of ZnO [1–4], while less attention has been paid to its mechanical properties.

Owing to the relatively poor mechanical performances of ZnO than other wide band gap semiconductors and the concern about the possible contact-induced damages which can be introduced during its device fabrication processes [6–8], mechanical properties as well as contact-induced deformation behaviour of this material have been investigated through nanoindentation [7–15]. Scope of previous nanoindentation studies has been mostly limited to the measurement of time-independent mechanical properties; for example, hardness (H) and elastic modulus (E) for (0 0 0 1) ZnO single crystals were reported to be 3.1–7.2 and 111–143 GPa, respectively [8–15]. Through quasi-static nanoindentation combined with atomic force microscopy, scanning electron microscopy, transmission electron microscopy or cathodoluminescence spectroscopy, some studies

*Corresponding author. Email: jijang@hanyang.ac.kr

have explored contact-induced deformation behaviours (such as pyramidal and basal slip) [7–9] or optical properties associated with plastic deformation [7,10,11].

An important mechanical behaviour that must be evaluated additionally is time-dependent permanent deformation (so-called creep), which possibly leads to failure during device operations under long-term stress condition. ZnO is considered as an active layer in transparent and flexible thin-film transistors and solar cells [16,17]. In addition, since the bulk or thin-film ceramic materials cannot accommodate large strain without failure, significant advance has been recently made in the flexible devices adopting single-crystalline low-dimensional materials (such as nanowires, nanorods and nanobelts) [18–20]. In these applications, operating environments result in each component of the device being placed under sustained stresses for a relatively long time and those components could be deformed by small but long-lasting stress through creep processes. In this regard, the basic information of small-scale creep behaviour in ZnO single crystal should be necessary for assessing long-term mechanical reliability.

Nanoindentation is a promising way to successfully investigate small-scale creep behaviour. Recently, Choi et al. [21,22] proposed that reasonable creep stress exponent value of nanocrystalline Ni could be obtained through constant load indentation creep tests with spherical indenter instead of commonly used Berkovich one. Similarly, in the present study, we have systematically investigated the creep behaviour of (0 0 0 1) single-crystal ZnO through spherical nanoindetation creep tests. By performing the constant load creep tests at the various load levels, we explore the yielding-induced transition in creep deformation mechanism.

2. Experimental

All experiments were performed on a 10 mm × 10 mm × 5 mm rectangular plate of a (0 0 0 1) ZnO single crystal purchased from Crystal Bank (Busan, Korea). Before tests, the sample surfaces were ultrasonically cleaned up in acetone, ethanol and then in deionized water for more than 30 min. Nanoindentation tests were conducted using a Nanoindenter-XP (formerly MTS-now Agilent, Oak Ridge, TN) equipped with a diamond spherical indenter. Indenter tip radius, R, was estimated as 5.883 μm by Hertzian contact analysis of the data obtained from indentations on fused quartz [23]. Constant load indentation creep test were performed with a spherical tip at various stresses in both elastic and elastic–plastic regimes (i.e. below and above the loads for "the first pop-ins" that correspond to yielding in spherical indentation). The specimens were loaded to various maximum load, P_{max}, at a fixed indentation strain rate of $P^{-1}(dP/dt) = 0.05/s$, held at P_{max} for 200 s, and fully unloaded.

3. Results

3.1. *P–h* curve

Figure 1(a) shows representative quasi-static nanoindentation load-displacement (P–h) curves obtained at a peak load of 80 mN. Sudden displacement excursions (often referred to as "pop-ins") were observed during the loading sequence, and the displacements were not fully recovered on unloading. In the figure, the P–h data recorded during indentation at lower P_{max} of 45 mN (below the pop-in load) are also exhibited, in which the loading part of the curve is completely reversed upon unloading, indicating

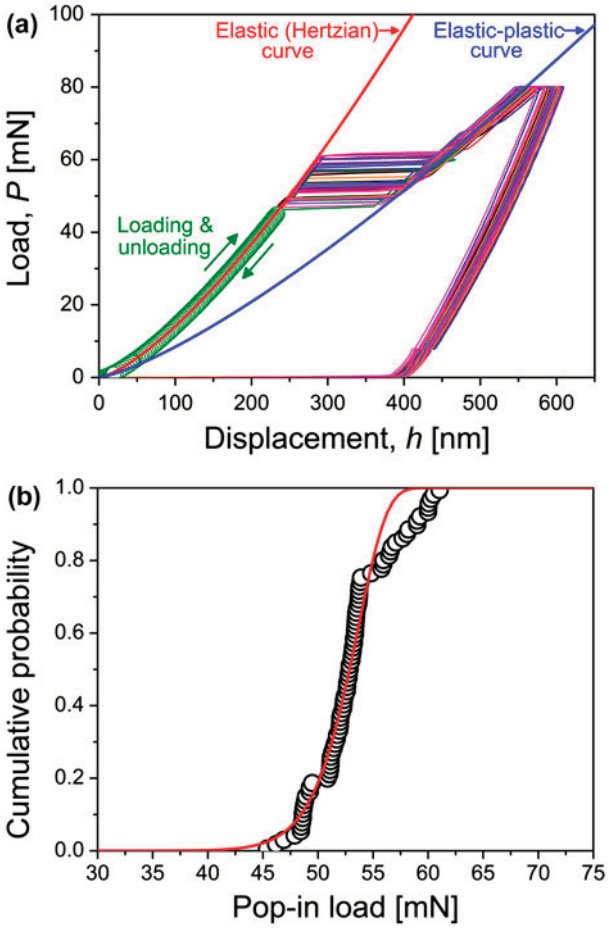

Figure 1. (colour online) The first pop-in behaviour observed in quasi-static spherical nanoindentation experiments; (a) load-displacement (P–h) curves exhibiting the pop-in behaviour and (b) cumulative probability distributions of the first pop-in loads.

that the deformation is purely elastic. Indeed the elastic P–h behaviour fits well with Hertzian elastic contact curve ($P = 4E_r\sqrt{R} \cdot h^{1.5}/3$ where R is the tip radius and E_r is the reduced modulus accounts for the fact that elastic deformations occur in both the indenter and the sample [23]). All these suggest that the pop-ins of ZnO single crystal also correspond to the elastic-to-plastic transition, as reported in the previous studies (e.g. see [24–26]). Although the first pop-in load varies in the range of ~45–61 mN (Figure 1(b)), the indenter displacement jumps from Hertzian curve to a unique elastic–plastic curve at the pop-in event, implying that the physical nature of the elastic-to-plastic transition does not vary with the load level.

As the first pop-in event is caused by the yielding, it is easy to define the applied creep loads for elastic and elastic–plastic regimes; i.e. P_{max} is set as below (5, 10, 20, 25, and 30 mN) and above (60, 70, 80, 90, and 100 mN) the first pop-in loads.

Figure 2(a) and (b) show representative P–h curves obtained from indentation creep tests performed in elastic and elastic–plastic regimes, respectively. In both regimes, the increase in h during load-hold sequence is clearly observed, suggesting that creep indeed occurs at room temperature. However, the creep behaviour is much more pronounced in elastic–plastic regime than in elastic regime, which will be discussed below. It is also noteworthy that creep displacement (h_{creep}) increases significantly with P_{max} in both regimes, indicating that the observed creep behaviour is realistic and not an artifact caused by thermal drift [22,27,28].

3.2. *Creep strain and creep rate*

As the first step to quantitatively analyse the creep behaviour, the indentation creep strain (ε_{creep}) is quantified as $\varepsilon_{creep} = 0.2(a - a_0)/R$ where a is the contact radius and

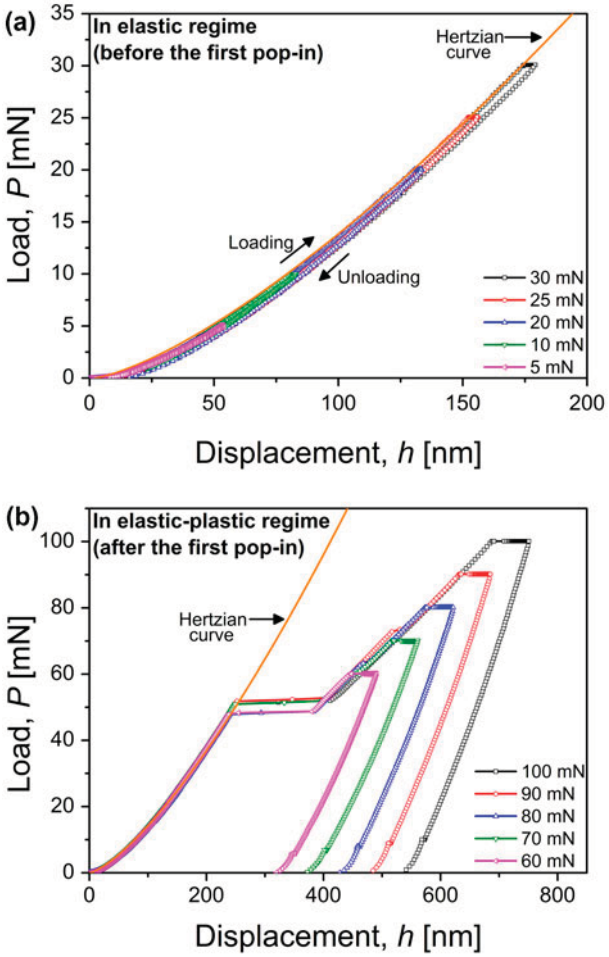

Figure 2. (colour online) Typical example of load-displacement curves obtained from indentation creep tests in (a) elastic strain and (b) elastic–plastic strain regimes.

a_0 is the contact radius at the onset of the creep. Here, a is estimated as $a = \sqrt{2hR - h^2}$ in simple consideration of contact geometry of spherical indentation. Note that in this study, measured h is used instead of precise value of contact depth h_c for the sake of simplicity. The calculation results are described in Figure 3(a) as a function of holding time ($t_{holding}$). The ε_{creep} vs. $t_{holding}$ curves are parabolic in nature, which are somewhat analogous to the typical high-temperature creep curves of metals and ceramics [29,30], consisting of two regimes in the early stages; transient and steady-state creep regimes. It is also noteworthy in the figure that, in both elastic and elastic–plastic regime, the amount of ε_{creep} is found to increase significantly with P_{max}. This clear load dependency of the ε_{creep} indicates that the observed creep behaviour is not an artifact caused by thermal drift which does not depend on load.

In Figure 3(b), the total creep strain and total creep displacement (determined as ε_{creep} and h_{creep} at $t_{holidng} = 200$ s, respectively) are plotted as a function of P_{max}. In the

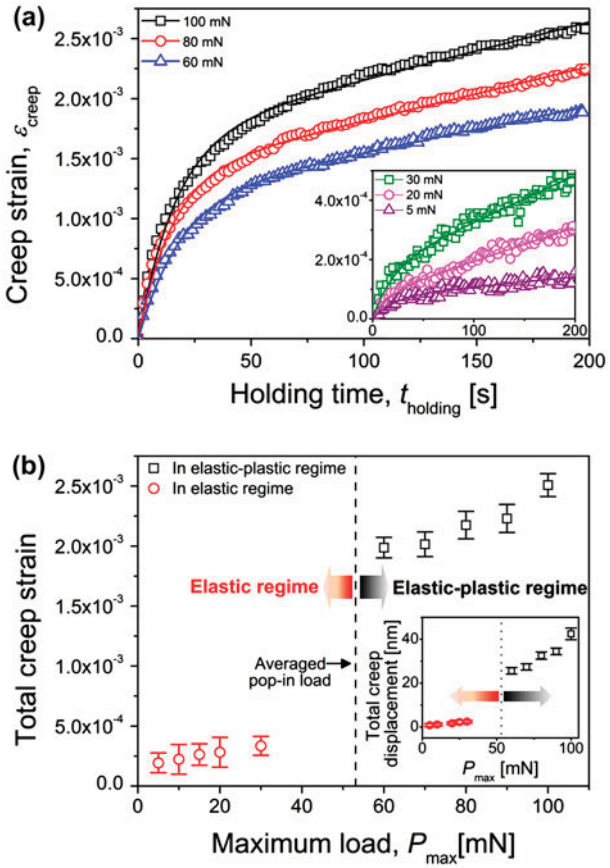

Figure 3. (colour online) Change in creep strain; (a) typical creep strain vs. holding time curves obtained in the elastic–plastic regime (with the inset showing the curves in elastic regime); (b) variation in total creep strain as a function of maximum load. The inset image of (b) exhibits the effect of maximum load on total creep displacement.

plots, the averaged first pop-in load value (~53 mN) is shown as vertical line, to demarcate elastic and elastic–plastic regimes of deformation. Both total creep strain and displacement in elastic regime are about one order of magnitude smaller than that in elastic–plastic regime. In other words, creep behaviour becomes much enhanced after pop-in occurs, conceivably suggesting there is transition of creep mechanism.

To estimate the indentation creep strain rates ($\dot{\varepsilon}_{creep}$), the ε_{creep} vs. $t_{holding}$ curves were fitted according to Garofalo's mathematical fitting equation, $\varepsilon - \varepsilon_0 = \varepsilon_{creep} = \alpha[1 - \exp(-rt_{holding})] + \chi t_{holding}$, where, ε is total strain including strain by instantaneous loading (ε_0) and creep (ε_{creep}), and α, χ and r are creep constants (for physical meanings of each parameters, see Ref. [21]). By differentiating the fitted equation with respect to $t_{holding}$, the change in $\dot{\varepsilon}_{creep}$ can be obtained as a function of $t_{holding}$. Typical examples of the determined $\dot{\varepsilon}_{creep}$ vs. $t_{holding}$ in elastic–plastic regime are plotted in Figure 4, suggesting the possibility of close approach to the steady-state condition, although it is theoretically implausible to reach the steady-state condition during indentation creep for 200 s. Thus, the condition is hereinafter called "quasi-steady-state." This condition is also observed in elastic regime in the inset of Figure 4. Figure 5 summarizes the variation in quasi-steady-state creep rate ($\dot{\varepsilon}_{QSS}$, defined as $\dot{\varepsilon}_{creep}$ at $t_{holi-dng} = 200$ s). Similar to the trends in Figure 3(b), higher $\dot{\varepsilon}_{QSS}$ values are evident for higher Pmax and $\dot{\varepsilon}_{QSS}$ values in elastic–plastic regime are one order of magnitude higher than those in elastic regime.

4. Discussion

Estimating the predominant creep mechanism is essential for better understanding of the creep behaviour in ZnO single crystal. A useful indicator of the creep mechanisms is the creep stress exponent n ($=\partial \log \dot{\varepsilon}_{SS} / \partial \log \sigma$) where $\dot{\varepsilon}_{SS}$ is the steady-state strain rate and σ is the applied creep stress during conventional uniaxial creep tests; i.e. $n = 1$ for diffusion creep such as the Nabarro–Herring creep (by lattice diffusion) or the Coble creep (by grain boundary diffusion), $n = 2$ for grain boundary sliding, $n = 3$–8 for

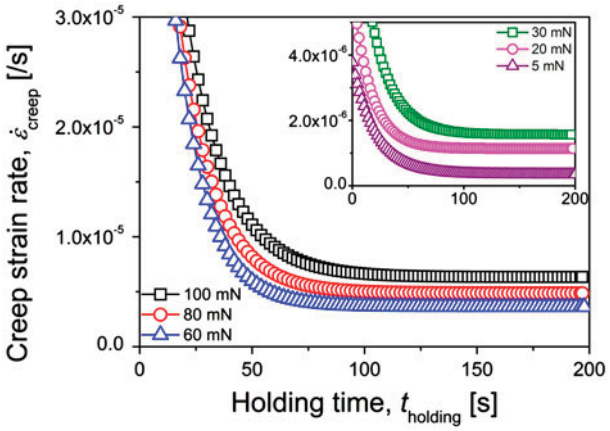

Figure 4. (colour online) Typical example of strain rate vs. holding time plots in the elastic–plastic regime. The inset shows the curves for the elastic regime.

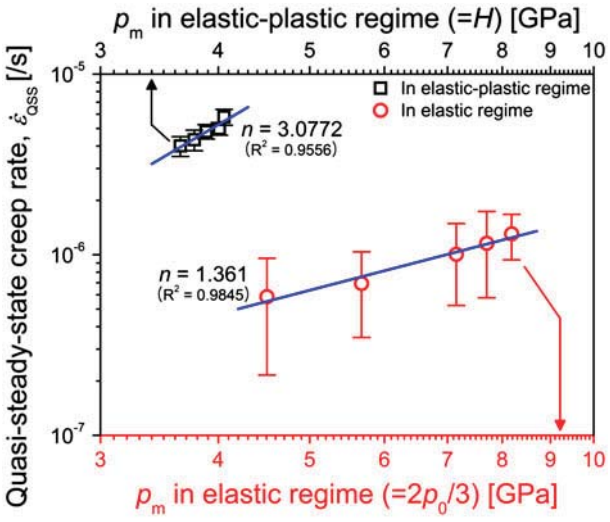

Figure 5. (colour online) Relations between quasi-steady-state strain rate and mean pressure, of which slope corresponds to the creep stress exponent, n.

dislocation creep in metals [29]. These creep mechanisms were originally developed for metals and alloys for high-temperature applications, but was found to be successfully extended to ceramics (where $n = 3$–5 for dislocation creep) [30]. Considering linear relations (1) between σ and the mean contact pressure p_m ($= P_{max}/\pi a_0^2$) at the onset of creep by Tabor's empirical law ($p_m = C\sigma$ where C is constraint factor) and (2) between the indentation quasi-static-state strain rate $\dot{\varepsilon}_{QSS}$ and the uniaxial steady-state strain rate $\dot{\varepsilon}_{SS}$ by empirical relation, $\dot{\varepsilon}_{SS} \sim 0.01\dot{\varepsilon}_{QSS}$ [22], the same n values can be obtained from $(\partial \log \dot{\varepsilon}_{QSS}/\partial \log p_m)$. According to Hertzian contact theory [23], for elastic contact where p_m is two-thirds of the maximum pressure ($2p_0/3$), the p_m can be determined with $a_{elastic} = (3P_{max}R/4E_r)^{1/3}$, in which E_r was calculated as $1/E_r = (1-\nu_{ZnO}^2)/E_{ZnO} + (1-\nu_i^2)/E_i$ where ν and E is Poisson's ratio and elastic modulus with subscript ZnO and i indicating the specimen and the indenter; $\nu_i = 0.07$ and $E_i = 1141$ GPa for diamond indenter [31] and $\nu_{ZnO} = 0.02$ and $E_{ZnO} = 111$ GPa for single-crystal ZnO [8]. However, this Hertzian equation cannot be extended into elastic–plastic regime and thus the p_m (i.e. hardness H) can be determined in consideration of contact geometry; $a_{plastic} = \sqrt{2hR - h^2}$ at the onset of creep. The relation of log ($\dot{\varepsilon}_{QSS}$) and log(p_m) and the obtained stress exponent n are shown in Figure 5. Linear fittings of the average points lead to the stress exponent $n \sim 1.361$ for elastic contact and ~3.077 for elastic–plastic contact, indicating the creep mechanism dominated by diffusion in elastic strain regime and by dislocation activities in elastic–plastic strain regime.

Room temperature creep behaviour of (11–20) ZnO single crystal was also reported by Basu et al. [32] who performed constant-stress spherical indentation creep tests at a load higher than the first pop-in load (i.e. at a load for elastic–plastic strain regime). Their obtained value of n (~3.1) is very similar to that obtained in elastic–plastic regime of the present study ($n \sim 3.077$). As reviewed by Cannon and Langdon [30], the n values in the literature reporting the dislocation creep in ceramic tend to group around

either $n \sim 3$ or ~5 and a larger proportion of the previous studies exhibits $n \sim 3$ as in the present study. This categorization of n has been explained by various factors. First, the ratio of the anion radius to cation radius (r_{anion}/r_{cation}) appears to be important [30,33,34]; e.g. the values of r_{anion}/r_{cation} for ceramics with $n \sim 3$ are 4.00 (for BeO), 2.64 (for Al_2O_3) and 1.94 (for MgO), and those with $n \sim 5$ are 1.78 (for NaCl), 1.31 (for KCl) and 1.40 (for CaO) [33–35]. According to Cannon and Sherby [33], high r_{anion}/r_{cation} values (> ~2) result in large polarizability of the constituent ions and dislocations to be strongly charged. In ionic materials, these dislocations will be dragged by charged defects (including vacancies, interstitials of ions and impurity atoms) during dislocation glide in creep deformation. In this regard, the fact that ZnO has the r_{anion}/r_{cation} of ~1.90 [35] (very close to that of MgO) may explain $n \sim 3$ in the elastic–plastic contact regime.

Another important parameter for determining n is the creep temperature [30,34]. Wilshire and Watkins [34] found $n \sim 3$ when creep temperature is lower than brittle-ductile transition temperatures and $n \sim 5$ when vice versa. They concluded that, while creep of ceramic with $n \sim 5$ may be associated with fully ductile conditions, that with $n \sim 3$ is usually observed in less ductile condition where crystallographic slip is restricted. In this sense, $n \sim 3$ in the elastic–plastic regime is also explained by the testing temperature lower than the transition temperature of ZnO.

While creep in elastic–plastic regime can be explained by dislocation mechanism supported by the increased dislocation density (on the pyramidal and basal slip planes after first pop-in [7–9]) in the highly stressed region underneath the indenter, the creep in elastic regime cannot be easily understood due to low diffusivity of lattice diffusion in single crystal at low homologous temperature (T/T_m) of ZnO where T_m is the absolute melting temperature (2273 K for ZnO [1]); i.e. room temperature corresponds to $T/T_m \sim 0.13$.

Only possible creep mechanism for the elastic contact is the diffusive flow along the interface between the indenter and surface of ZnO single crystal. The tip-sample interface provides a faster diffusion path than lattice [36,37]. The interface diffusion may play more important role in shallow-depth regime as discussed by Wang et al. [36]. In addition, diffusion creep behaviour ($n \sim 1$) was clearly observed in the authors' previous study on compression creep of single-crystal ZnO nanorods (with equivalent diameter of ~200–2000 nm) [27]. In the study, more pronounced creep behaviour was observed in smaller nanorods and this size effect on creep behaviour was explained by higher fraction of surface (and interface between flat-punch tip and sample surface) to volume in smaller nanorods. At room temperature, surface diffusivity (D_{surf}) of Zn or O ions is much higher than their lattice diffusivity ($D_{lattice}$) as $D_{surf}/D_{lattice}$ of $\sim 10^{12}$ for Zn and $\sim 10^{15}$ for O [27], suggesting the possible occurrence of diffusion creep through surface.

The strain-dependent transition of creep mechanism introduced above may be due to the abrupt increase in dislocation density by pop-in phenomena (and possibly the increased diffusion path – dislocation core – for ions). Although similar pop-in-induced transition of creep behaviour have been reported in various materials (such as Al [38,39], Ni_3Al [39], fused quartz [39], W [40], GaAs [40], Cu [41] and In [38]), their transitions are somewhat different from our observation. For example, Wang and Xu [41] performed indentation creep tests in plastic regime on polycrystalline Cu thin film and reported that, after pop-in occurs during load-hold sequence, n was decreased from

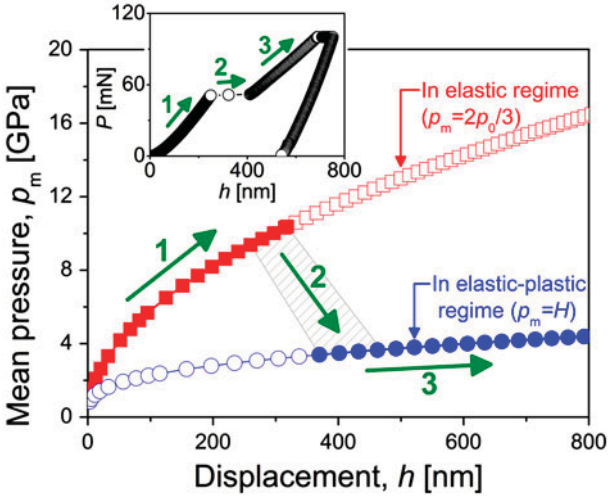

Figure 6. (colour online) Variation in mean contact pressure as a function of indentation displacement. Shaded region indicates the transition of mean pressure by the first pop-in at ~45–61 mN. The inset shows the corresponding P–h curve (for $P_{max} = 100$ mN case in Figure 2(b)).

8.4 to 6.3, both corresponding to dislocation-dominated creep mechanism. Only Feng and Ngan [38] found pop-in-induced transition of creep mechanism from diffusion ($n \sim 1.5$) to dislocation ($n \sim 6$) after the first pop-in, in the low-melting materials of In and suggested that crystal plasticity will alter the mechanism of indentation creep, which is in agreement with our results.

In Figure 5, it is interesting that, while the p_m increases with P_{max} in both elastic and elastic–plastic regime, the p_m at the onset of creep is much higher in elastic regime than in elastic–plastic regime. It is noteworthy that the absolute values of p_m for the elastic contact may not be directly compared with that for the elastic–plastic contact. This is because the pressure distribution for elastic–plastic contact (whose general solution has not been established by far) must be more homogeneous than the simple Hertzian pressure distribution. The reason for the difficulty in direct comparison is also captured in Figure 6 where an example of the change in calculated p_m during loading is traced with h, which corresponds to the P–h curve of $P_{max} = 100$ mN in Figure 2(b), as shown in the inset. As h increases, p_m increases rapidly along the p_m–h curve of elastic regime (arrow "1" in the figure), drops abruptly at the first pop-in (arrow "2") and then increases again along the curve of elastic–plastic regime (arrow "3"). A similar drop of p_m at the first pop-in was also reported by Basu et al. [9] who performed spherical indentation tests on ZnO single crystal.

5. Conclusions

Creep behaviour of (0 0 0 1)-oriented ZnO single crystal has been systematically investigated through spherical indentation creep tests in both elastic and elastic–plastic contact regimes. While it was revealed that creep indeed occurs at ambient temperature in both regimes, the creep plasticity was more pronounced in the elastic–plastic strain regime.

The creep stress exponent n, estimated from quasi-steady-static strain rate and mean pressure, suggested the strain-dependent transition of creep mechanism from possible diffusion in elastic regime ($n \sim 1.361$) to dislocation activities in elastic–plastic ($n \sim 3.077$) regime, respectively. This transition was analysed in consideration of possible factors affecting the creep in each regime.

Funding

This research was supported in part by the National Research Foundation of Korea (NRF) grant funded by the Korea government (MSIP) [grant number 2013R1A1A2A10058551], and in part by the Human Resources Development program of the Korea Institute of Energy Technology Evaluation and Planning (KETEP) grant funded by the Korea government (MOTIE) [grant number 20134030200360].

References

[1] Ü. Özgür, Y.I. Alivov, C. Liu, A. Teke, M.A. Reshchikov, S. Doğan, V. Avrutin, S.J. Cho and H. Morkoc, J. Appl. Phys. 98 (2005) p.041301.
[2] C. Klingshirn, Phys. Status Solidi B 244 (2007) p.3027.
[3] A. Janotti and C.G. Van de Walle, Rep. Prog. Phys. 72 (2009) p.126501.
[4] A.B. Djurišić and Y.H. Leung, Small 2 (2006) p.944.
[5] Z.L. Wang, MRS Bull. 37 (2012) p.814.
[6] I. Yonenaga, H. Koizumi, Y. Ohno and T. Taishi, J. Appl. Phys. 103 (2008) p.093502.
[7] J.E. Bradby, S.O. Kucheyev, J.S. Williams, C. Jagadish, M.V. Swain, P. Munroe and M.R. Phillips, Appl. Phys. Lett. 80 (2002) p.4537.
[8] S.O. Kucheyev, J.E. Bradby, J.S. Williams, C. Jagadish and M.V. Swain, Appl. Phys. Lett. 80 (2002) p.956.
[9] S. Basu and M.W. Barsoum, J. Mater. Res. 22 (2007) p.2470.
[10] S.-R. Jian, J. Alloys Compd. 494 (2010) p.214.
[11] R. Juday, E.M. Silva, J.Y. Huang, P.G. Caldas, R. Prioli and F.A. Ponce, J. Appl. Phys. 113 (2013) p.183511.
[12] D.A. Lucca, M.J. Klopfstein, R. Ghisleni and G. Cantwell, CIRP Ann. Manuf. Technol. 51 (2002) p.483.
[13] J.E. Bradby, J.S. Williams and M.V. Swain, J. Mater. Res. 19 (2004) p.380.
[14] V.A. Coleman, J.E. Bradby, C. Jagadish, P. Munroe, Y.W. Heo, S.J. Pearton, D.P. Norton, M. Inoue and M. Yano, Appl. Phys. Lett. 86 (2005) p.203105.
[15] R. Navamathavan, S.-J. Park, J.-H. Hahn and C.K. Choi, Mater. Charact. 59 (2008) p.359.
[16] K. Song, J. Noh, T. Jun, Y. Jung, H.-Y. Kang and J. Moon, Adv. Mater. 22 (2010) p.4308.
[17] X. Wen, W. Wu, Y. Ding and Z.L. Wang, Nano Energy 2 (2013) p.1093.
[18] J.M. Lee, J.W. Choung, J. Yi, D.H. Lee, M. Samal, D.K. Yi, C.-H. Lee, G.-C. Yi, U. Paik, J.A. Rogers and W.I. Park, Nano Lett. 10 (2010) p.2783.
[19] Z.L. Wang, MRS Bull. 37 (2012) p.814.
[20] Y.-J. Kim, K. Son, I.-C. Choi, I.-S. Choi, W.I. Park and J.-I. Jang, Adv. Funct. Mater. 21 (2011) p.279.
[21] I.-C. Choi, B.-G. Yoo, Y.-J. Kim and J.-I. Jang, J. Mater. Res. 27 (2012) p.3.
[22] I.-C. Choi, B.-G. Yoo, Y.-J. Kim, M.-Y. Seok, Y. Wang and J.-I. Jang, Scr. Mater. 65 (2011) p.300.
[23] K.L. Johnson, *Contact Mechanics*, Cambridge University Press, Cambridge, 1985.
[24] T.F. Page, W.C. Oliver and C.J. McHargue, J. Mater. Res. 7 (1992) p.450.

[25] I.-C. Choi, Y. Zhao, Y.-J. Kim, B.-G. Yoo, J.-Y. Suh, U. Ramamurty and J.-I. Jang, Acta Mater. 60 (2012) p.6862.
[26] J.-I. Jang, H. Bei, P.F. Becher and G.M. Pharr, J. Am. Ceram. Soc. 95 (2012) p.2113.
[27] Y.-J. Kim, W.W. Lee, I.-C. Choi, B.-G. Yoo, S.M. Han, H.G. Park, W.-I. Park and J.-I. Jang, Acta Mater. 61 (2013) p.7180.
[28] B.-G. Yoo, K.-S. Kim, J.-H. Oh, U. Ramamurty and J.-I. Jang, Scr. Mater. 63 (2010) p.1205.
[29] G.E. Dieter, *Mechanical Metallurgy*, McGraw-Hill, London, 1988.
[30] W.R. Cannon and T.G. Langdon, J. Mater. Sci. 23 (1988) p.1.
[31] W.C. Oliver and G.M. Pharr, J. Mater. Res. 7 (1992) p.1564.
[32] S. Basu, M. Radovic and M.W. Barsoum, J. Appl. Phys. 104 (2008) p.063522.
[33] W.R. Cannona and O.D. Sherby, J. Am. Ceram. Soc. 56 (1973) p.157.
[34] B. Wilshire and B. Watkins, J. Mater. Sci. 12 (1977) p.2135.
[35] W.D. Callister, *Fundamentals of Materials Science and Engineering: An Integrated Approach*, Wiley, New York, 2005.
[36] F. Wang, P. Huang and T. Lu, J. Mater. Res. 24 (2009) p.3277.
[37] W.B. Li and R. Warren, Acta Metall. Mater. 41 (1993) p.3065.
[38] G. Feng and A.H.W. Ngan, Scr. Mater. 45 (2001) p.971.
[39] H. Li and A.H.W. Ngan, J. Mater. Res. 19 (2004) p.513.
[40] S.A. Syed Asif and J.B. Pethica, Philos. Mag. 76 (1997) p.1105.
[41] F. Wang and K. Xu, Mater. Lett. 58 (2004) p.2345.